Moroccan Journal of Chemistry
ISSN: 2351-812X
http://revues.imist.ma/?journal=morjchem&page=login
Asep Bayu Dani Nandiyanto / Mor. J. Chem. 8 N°3 (2020) 745-761

Isotherm Adsorption of Carbon Microparticles Prepared from Pumpkin (*Cucurbita maxima*) Seeds Using Two-Parameter Monolayer Adsorption Models and Equations

Asep Bayu Dani Nandiyanto

Departemen Kimia, Universitas Pendidikan Indonesia, Jl. Setiabudi No. 229, Bandung, Indonesia

* *Corresponding author:*
nandiyanto@upi.edu
Received 12 April 2019,
Revised 25 June 2020,
Accepted 28 Jun 2020

Abstract

The isotherm adsorption of carbon microparticles prepared from pumpkin (*Cucurbita maxima*) seeds were studied and modelled. Experiments were done by evaluating carbon microparticles with various sizes (from 100 to 1000 um) for adsorbing curcumin (as a model of adsorbate) in an aqueous solution, and the results were derived and compared using the kinetics approach based on several standard isotherm adsorption models. Seven isotherm models were used to predict and determine the characteristic parameters: Langmuir, Freundlich, Temkin, Dubinin-Radushkevich, Flory-Huggins, Fowler–Guggenheim, and Hill-de Boer isotherm models. The results were then analyzed and accompanied by an adequate explanation related with the adsorption mechanisms and the determination techniques of its adsorption constants. The models showed that the interaction of adsorbates with carbon surface is done in multilayers with physical processes. Inorganic contents in the pumpkin seeds allow the formation of carbon with porosities, making more sites for the adsorption. The adsorbed molecules attract and associate with other free molecules. The adsorption is carried out on energetically different sites under an endothermic process. The Gibbs free energy confirmed that the adsorption is spontaneous. The results also confirmed that smaller adsorbent have direct impacts on the improving adsorption capacity (due to the existence of large surface area). Small-sized adsorbent (sizes < 500 um) has better additional adsorption (due to adsorbate-adsorbate interaction and possible existence of chemical interaction), resulting in the boosting adsorption capacity. This study is useful for further developments of carbon microparticles from organic waste material.

Keywords: *economic perspective; engineering perspective; agricultural wastes; silica; economic parameter..*

1. Introduction

Carbon is one of the important elements in nature and can be classified as the fourth most abundant element in universe [1, 2]. Carbon has been used in various applications due to its excellent performance[3]. To produce carbon, one of the most prospective raw materials is organic waste, such as orange skin [4], rice husk and rice straw [5-9], tea leave waste [10], dragon fruit peel [11], walnut shells [12], pumpkin seed shell [3, 13], palm shells[14], coconut shell[15], and Mangosteen peel[16]. The use of waste is important for transforming waste into useful product[16]. Here, different from other reports regarding the synthesis of carbon particles, the main objective of this study was to analyze the isotherm adsorption of carbon microparticles from pumpkin seed waste. The adsorption ability of carbon was compared with several standard isotherm adsorption models: Langmuir, Freundlich, Temkin, Dubinin-Radushkevich, Flory-Huggins, Fowler–Guggenheim, and Hill-de Boer isotherm models. Although many papers have reported the study on the adsorption profile[6, 8, 9, 16-19], this report is completed with theoretical explanation and modelling, as well as illustration for the phenomena happening during the adsorption process. The first originality in this study is the use of carbon from pumpkin seed waste. Pumpkin seed was the main focus as the carbon source since it has high amount of carbon components. Pumpkin seed is one of the most product commodities in the world[20]. For example, Australia exported approximately 130,000 ton annually to Japan[21]. Usually, pumpkin is sold without the seeds, while the seeds are disposed without further considerations. In fact, pumpkin seeds can grow as weeds in farm. When they decomposed, bad odor or smell can be created[22]. Understanding strategy for transforming pumpkin seeds into better products such as carbon is important for solving issues in the boosting number of pumpkin seeds waste, especially in Indonesia. The second originality is the evaluation of isotherm adsorption of carbon microparticles with various particle sizes (from 100 to 1000 um). Particle size correlates to the number of surface active sites (the main place for the adsorption process). Indeed, by understanding this parameter, adsorption phenomena happening on the carbon particles can be predicted, giving suggestions for further applications (such as catalyst and adsorbent) of carbon materials from pumpkin seeds. The third originality is the use of curcumin as a model of dye. Curcumin was selected because it has an ideal molecular size (less than 1.4 nm)[9], which is perfect for evaluating adsorbent-adsorbate interaction and making it possible for predicting other types of organic adsorptives. In the fourth originality, while most of the studies typically focused on the evaluation of nanoparticles, this study emphasized the analysis of microparticles. Micrometer-sized particles are interested since they have excellent characteristics compared to nanoparticles, bulk, and film materials. They are easily settled and decanted spontaneously. This makes carbon microparticles separated easily after using, allowing them to be reusable. Further, their settling ability promotes them for not contaminating the sample for analysis, avoiding misleading measurement as well as giving precise evaluation and analysis.

2. Isotherm Adsorption Models Used in This Study

2.1. Adsorption Efficiency

The simplest analysis usually used in the adsorption process is the adsorption efficiency (η), which is measured using

$$\eta = \left(\frac{C_o - C_e}{C_o} \right) \times 100\% \qquad (1)$$

where C_o is the initial concentration of adsorbate (mg/L). C_e is the concentration of adsorbate equilibrium (mg/L).

2.2. Langmuir isotherm

The Langmuir model assists quantitative analysis for the formation of the monolayer adsorption model on the outer surface of the adsorbent. When the adsorbates attach the surface of adsorbent, no more adsorption process from other

adsorbates happens[23]. The Langmuir isotherm model also assumes the adsorption on homogeneous surfaces without interactions between adsorbate molecules (See **Figure 1(a)**). No transmigration from adsorbates happens during the adsorption process. The Langmuir model is predicted using[24]:

$$\frac{1}{q_e} = \frac{1}{q_m.K_L}\frac{1}{C_e} + \frac{1}{q_m} \quad (2)$$

$$R_L = \frac{1}{1+K_L C_e} \quad (3)$$

where K_L is the constant in the Langmuir model. q_e is the amount of molecules adsorbed per gram at equilibrium (mg/g) and q_m is the monolayer adsorption capacity (mg/g). R_L is the adsorption factor, describing [9]

(i) $R_L > 1$ is the unfavorable adsorption process (encouraging desorption)

(ii) $R_L = 1$ is the linear adsorption process (adsorption isotherms depend on the amount and concentration of adsorbed).

(iii) $R_L = 0$ is the irreversible adsorption process (too strong adsorption)

(iv) $0 < R_L < 1$ is the favorable adsorption process (adsorption can be controlled under certain conditions).

2.3. Freundlich isotherm

The Freundlich isotherm adsorption model is the most widely used non-linear adsorption model, which is under multilayer adsorption with a heterogeneous energetic distribution from the active site on the adsorbent[24]. This model also calculates the interactions between adsorbed molecules[25]. Multilayer adsorption can be applied in this isotherm model[9]. The adsorption energy is a function of the adsorption process on the adsorbent, which is expressed:

$$\ln q_e = \ln K_F + \frac{1}{n}\ln C_e \quad (4)$$

where K_F is the Freundlich constant as the estimated indicator of adsorption capacity. n is the adsorption intensity, which can predict the adsorption process using the following phenomena[5]:

(i) $n < 1$ is for the chemical adsorption (see **Figure 2(b)**)

(ii) $n = 1$ is for the linear adsorption (adsorption depends on the amount and concentration of adsorbed. It can be combination of chemical and physical adsorption processes)

(iii) $n > 1$ is the physical adsorption (see **Figure 2(a)**)

(iv) $1 / n < 1$ is the normal adsorption

(v) $1 / n > 1$ is the cooperative adsorption

(vi) $1 < 1 / n < 0$ is the favorable adsorption process (inhibiting the desorption process).

(vii) $0 < 1 / n < 1$ is the normal adsorption (can be controlled under certain conditions).

(viii) If $1/n$ is near to zero, the surface of adsorbent is more heterogeneous.

2.4. Temkin isotherm

The Temkin model discusses the correlation of indirect adsorbate interactions and the isotherm adsorption. The heat of adsorption of all adsorbate molecules in the layer is a function of adsorbate-adsorbate interactions [26]. The model describes a factor that is explicitly in the adsorbate interaction condition. By adding assumption in the use of very low concentrations of adsorbates, the heat of adsorption from all molecules in the layer is a function of temperature as expressed by[9]:

$$q_e = B_T(\ln C_e) + (B_T \ln A_T) \quad (5)$$

where A_T is the equilibrium constant in the Temkin isotherm model. B_T is the Temkin's isotherm constant, explaining that:

(i) B_T < 8 kJ shows the physical adsorption

(ii) B_T > 8 kJ shows the chemical adsorption

The Temkin model also can predict involvement of energy in the adsorption process:

$$\theta = \frac{RT}{\Delta Q}\ln(C_e) + \frac{RT}{\Delta Q}\ln(K_T) \quad (6)$$

where T is the absolute temperature (K) and R is the Boltzmann gas constant (8.314 J/mol.K). θ is the fraction of adsorbed components on the surface of adsorbent, which can be estimated by dividing adsorbed adsorbates on the surface of adsorbent with total amount of initial concentration of adsorbates. K_T is the energy constant (L/mg) in Temkin. ΔQ is the adsorption energy (kJ/mol). Assuming that the process is done under close system, the value of ΔQ is almost identical with the heat (ΔH), resulting

$$\Delta Q = -\Delta H \quad (7)$$

The value of ΔH can be described as : ΔH > 0 kJ/mol is the endothermic processes. And ΔH < 0 kJ/mol is the exothermic processes.

2.5. Dubinin-Radushkevich isotherm

The Dubinin-Radushkevich model is generally applied to regulate the mechanism of adsorption based on heterogeneous surfaces[26]:

$$\ln q_e = \ln q_s - \beta\varepsilon^2 \quad (8)$$

where q_s is the saturation capacity of theoretical isotherms (mg/g), β is the Dubinin-Radushkevich isotherm constant relating to the average free adsorption energy per mol of adsorbate, and ε is the Polanyi potential associated with the equilibrium condition. This model correlates to the following equations:

$$\varepsilon = RT\ln\left[1 + \frac{1}{C_e}\right] \quad (9)$$

$$E = \frac{1}{\sqrt{2\beta}} \quad (10)$$

where E is the energy for predicting type of adsorption: E < 8 kJ / mol is the physical adsorption and E > 8 kJ / mol is the chemical adsorption

2.6. Flory-Huggins isotherm

The Flory-Huggins isotherm model is occasionally used for understanding degree of surface coverage characteristics of adsorbate onto surface of adsorbent. This model expresses the feasibility and spontaneous phenomena in the adsorption process[27]. The equation of Flory-Huggins isotherm is presented:

$$\frac{\theta}{C_O} = K_{FH}(1-\theta)^{nFH} \quad (11)$$

where nFH is the number of adsorbate molecules occupying on the sorption sites on the surface of adsorbent. K_{FH} is the equilibrium Flory-Huggins constant.

2.7. Fowler–Guggenheim isotherm

The Fowler–Guggenheim takes the lateral interaction of the adsorbed molecules during the adsorption process. The model is one of the simplest correlations allowing for the prediction in the lateral interaction between adsorbates[28]. This model is explicitly explained:

$$K_{FG}.C_e = \frac{\theta}{1-\theta}\exp\left(\frac{2.\theta.W}{R.T}\right) \quad (12)$$

where K_{FG} is the Fowler–Guggenheim equilibrium constant (L/mg). W is the interaction energy between adsorbed molecules (kJ/mol), in which the value of W correlates with the heat of adsorption. The heat varies linearly with loading adsorbed molecules on the surface of adsorbent.

(i) $W > 0$ kJ/mol is the attraction between adsorbed molecules, and the existence of exothermic processes.

(ii) $W < 0$ kJ/mol is the repulsion between adsorbed molecules, and the existence of endothermic processes.

(iii) $W = 0$ kJ/mol is no interaction between adsorbed molecules.

2.8. Hill-de Boer isotherm

The Hill–de Boer isotherm model explains about mobile adsorption and lateral interaction among adsorbed molecules[28]. The model is approximated using

$$K_1.Ce = \frac{\theta}{1-\theta}\exp\left(\frac{\theta}{1-\theta} - \frac{K_2\theta}{RT}\right) \quad (13)$$

where K_1 is the Hill–de Boer constant (L/mg) and K_2 is the energetic constant of the interaction between adsorbed molecules (kJ/mol).

(i) $K_2 > 0$ kJ/mol is the attraction between adsorbed molecules.

(ii) $K_2 < 0$ kJ/mol is the repulsion between adsorbed molecules.

(iii) $K_2 = 0$ kJ/mol is no interaction between adsorbed molecules.

2.9. Gibbs free energy

This energy is used for predicting the type of energy happening during the adsorption process[29]. The Gibbs free energy (ΔGf) predicts the spontaneity of the adsorption process, which is estimated using:

$$\Delta Gf \approx -RT \ln K_X \quad (14)$$

where K_X is the adsorption constant based on isotherm models, such as K_L, K_f, K_2, K_{FG}, and K_{FH}. The Gibbs free energy defines:

(i) $\Delta Gf > 0$ kJ/mol is the non-spontaneous adsorption.

(ii) $\Delta Gf < 0$ kJ/mol is the spontaneous adsorption.

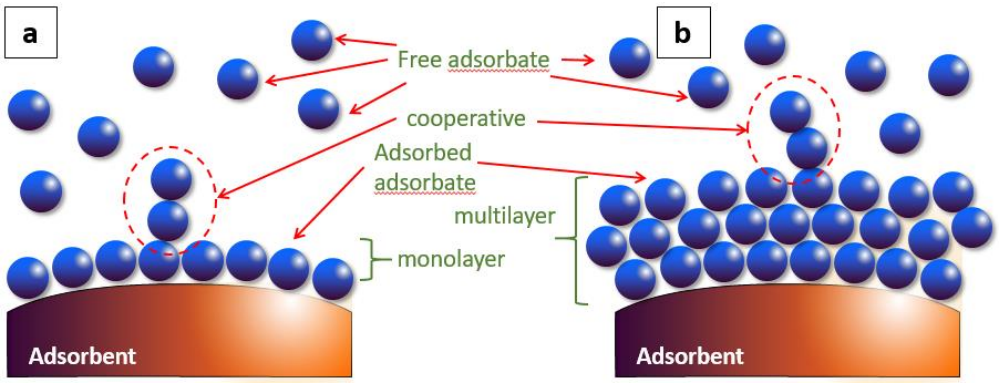

Figure 1. Illustration of adsorption process under monolayer (a) and multilayer (b).

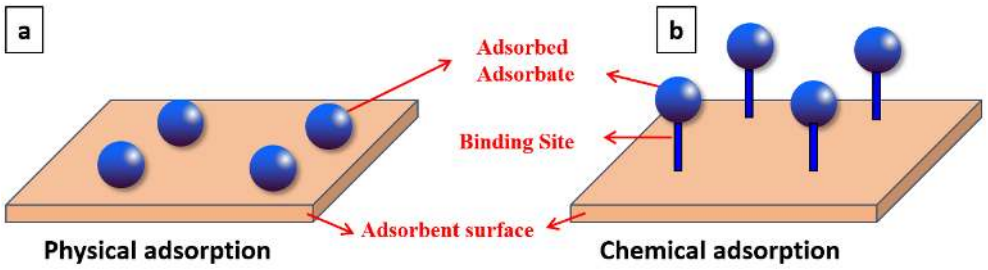

Figure 2. Illustration of interaction between adsorbate and adsorbent surface. Figures (a) and (b) are the physical (a) and the chemical (b) adsorption.

3. Method

3.1. Preparation of Carbon Microparticles as Adsorbent

Illustration process in the production of carbon microparticles is depicted in **Figure 3**. Carbon microparticles were produced from pumpkin (*Cucurbita maxima*) seed waste. This waste was taken from Lembang, Indonesia, washed, dried at 100°C, and ground using a saw-milling apparatus. The saw-milled pumpkin seeds were dried and carbonized at 250°C for 2 hours in an electrical furnace, forming carbon. The formed carbon was then put into the saw-milling process (for getting fined microparticles). The experimental procedure for the saw-milling process is described in our previous reports[30].

3.2. Charaterizations for the Physicochemical Properties of the Carbon Microparticles

Several characterizations of the prepared carbon microparticles were used: a Fourier Transform Infrared (FTIR, FTIR-4600, Jasco Corp, Japan; for analyzing chemical component), a digital microscope (BXAW-AX-BC, China; for analyzing particle size), and a sieve test apparatus (Rumah Publikasi Indonesia, Indonesia; hole sizes of 2000, 1000, 841, 700, 595, 500, 250, 200, 125, 100, 74, 55 um; for classifying and analyzing particle size distribution) were used. The sieve test was also used for obtaining particles with specific sizes. Then, prior to using further analysis, the carbon microparticles with specific sizes were washed using centrifugation process (11,000 rpm; 5 min; washed by ultrapure water).

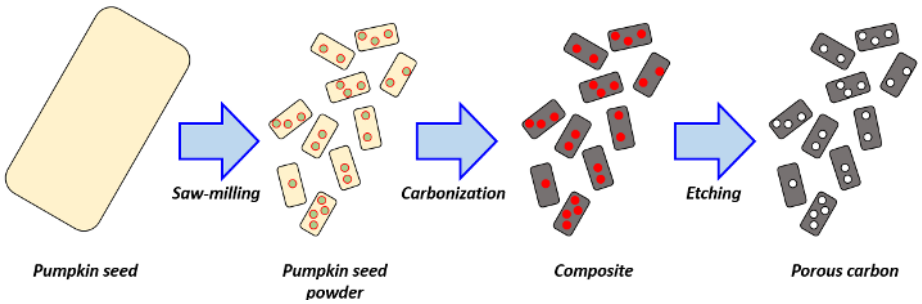

Figure 3. Illustration for the production of carbon microparticles

3.3. Isotherm Adsorption Analysis

The isotherm adsorption test was conducted by mixing 0.05 g of the prepared carbon microparticles with specific sizes (i.e. 200, 500 and 1000 um) into 100 mL of curcumin solution (concentration of 10, 30, and 50 ppm) in a batch-type adsorption apparatus (a 400-mL borosilicate batch glass having dimensions of 8 and 10 cm for diameter and height, respectively; equipped with a magnetic stirrer (1000 rpm)) for 20 minutes at room temperature and pressure. The

adsorption process was done in the close system to ensure no light and no oxidation since curcumin is reactive. Curcumin solution was prepared by extracting Turmeric (*Curcuma Longa*; obtained from local market in Bandung, Indonesia) using our previous method [31]. The adsorption profile was obtained by taking an aliquot (2-3 mL) in every 5 minutes from the adsorption apparatus, putting into the syringe filter (pore size of 220 nm), measuring the absorbance using a Visible Spectroscope (Model 7205; JENWAY; Cole-Parner; AS; at wavenumber of between 200 and 600 nm), plotting and normalizing the spectroscope results, and calculating using the Beer law analysis. The obtained data (concentration versus time) based on the Beer Law was then plotted and compared with the standard isotherm adsorption models: Langmuir, Freundlich, Temkin, Dubinin-Radushkevich, Flory-Huggins, Fowler–Guggenheim, and Hill-de Boer isotherm models.

4. Results

4.1. Physicochemical properties of the carbon microparticles

Figure 4(a) shows the microscope image of carbon microparticles. The Ferret analysis showed that the sizes of particles were in the range of between 55 and 2000 um. The particle size distribution results using a sieve test is shown in **Figure 4(b)**, identifying most of the particle sizes in the range of 200 and 1000 um, and giving information for the mean particle size of 195 um. The particles with different sizes were then classified and used for further adsorption analysis. **Figure 5** is the FTIR analysis results of carbon microparticles with various sizes.

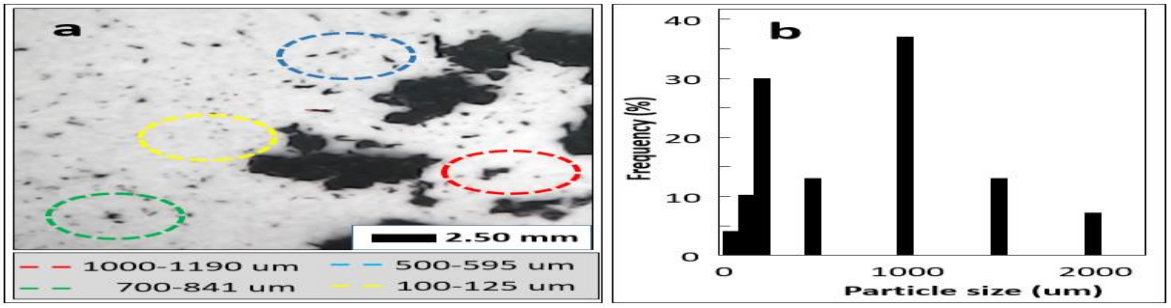

Figure 4. Microscope image (a) of carbon particles prepared from pumpkin seed waste with their particle size distribution (b)

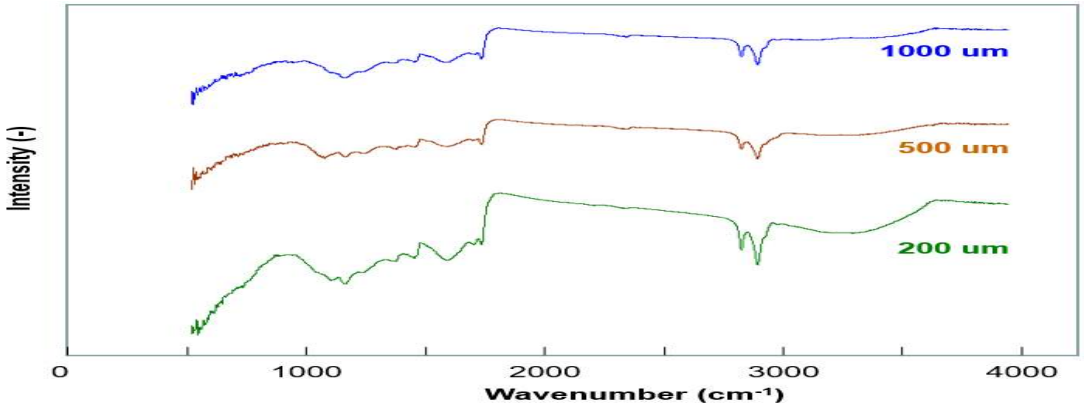

Figure 5. The FTIR analysis results of carbon particles with various sizes

All carbon sizes have identical FTIR peaks and patterns, replying that the process successfully transformed organic components into carbon material[32]. The FTIR analysis has four strong peaks. Peaks at 1225 (for aromatic C-H), 1600 (for conjugated C=C in olefin structure and alkene), 2845 (for symmetric C-H), and 2970 (asymmetric alkyl)

[32]. The FTIR analysis confirmed that the present samples are carbon material. No other peaks and patterns (which can be from inorganic components) in the FTIR analysis were detected, promoting the effectiveness in the etching process for removing inorganic components from the carbon material without additional reactions

4.2. Adsorption characteristics of carbon microparticles based on isotherm models

Figure 6 presents the correlation between efficiency and concentration of adsorbate under various sizes of carbon microparticles as adsorbent. All data agreed that the efficiency in adsorbing molecules depended on the particle sizes. The regression results from the data have almost identical gradient, but the intercept was different. Different values of intercepts are due to the effect of surface area on the adsorbent, in which smaller adsorbent sizes have larger surface area. To investigate the model of adsorption, experimental data were analyzed by a regression analysis to fit the linearized expression of mathematical models. The experimental values based on the plotting some parameters are reconstituted (using plot equations in **Table 1**). Experimental results (as points) and the theoretical calculated results (as lines) were plotted as presented in **Figures 7-13**. Linear correlation coefficients (r^2) are then used to show the compatibility of correlation curves between experimental data and linearized forms of the isotherm models. The plotting analysis can also derive several parameters in the adsorption process and predict what phenomena happening during the adsorption process[9]. Parameters obtained from the plotting analysis is presented in **Table 2**.

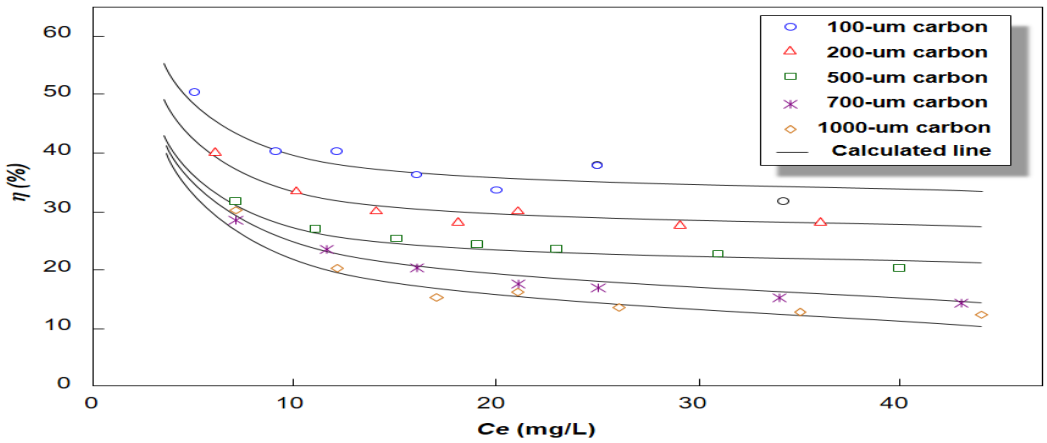

Figure 6. Comparison of experimental and predicted efficiency of adsorption of carbon microparticles.

Figure 7 shows the plotting analysis based on the Langmuir model. Plotting analysis showed that the carbon microparticles with sizes of 1000 and 700 um have R^2 values of 0.6081 and 0.8611, respectively, and that with smaller sizes (less than 500 um) have R^2 of more than 0.90. This informs that the adsorption process using the present carbon microparticles of less than 500 um have the potential for the formation of monolayer structure. The maximum adsorption capacities as q_m of carbon particles increased when using smaller carbon sizes. The R_L analysis showed the values in the range of between 0 and 1 for all sizes, informing the characteristics of carbon microparticles in the favorable condition, in which the adsorption process can be controlled by changing process condition. Analysis of ΔGf informed that all processes were done spontaneously for all carbon sizes. **Figure 8** shows the plotting analysis based on the Freundlich model. Plotting analysis showed that the R^2 values of carbon particles with sizes of 1000 um and less than 700 um were 0.80 and greater than 0.93, respectively. The values of R^2 in the Freundlich model for particles with sizes of less than 500 um are the highest compared to that in the other models, informing that the adsorption profile of carbon microparticles with sizes of less than 500 um fitted with the Freundlich model (having multilayer structure in the adsorption process). Analysis of n value for carbon microparticles showed the correlations of $n > 1$ and

$1/n < 1$, gving results that adsorption occurs physically with a favorable process. However, for the case of particles with sizes of 700 um, they have n value of less than 1. We also found that the cooperative process did not happen, informing that the multilayer is not due to the interaction between adsobate molecules. **Figures 9 and 10** are the plotting analysis results based on the Temkin model. R^2 values were varied. This model is good with enough R^2 values for carbon with sizes of 500 um. However, for other sizes, the R^2 values were less than 0.90, informing that this model is not fit. The B_T values showed that the carbon microparticles with sizes of less than 500 um involved chemical interaction, whearas carbon with larger sizes interfered physical interaction.

Table 1. Isotherm models and their linear form

Isotherm adsorption model	Initial equation	Linear form	Plot
Langmuir	$q_e = \frac{q_m.K_L.C_e}{1+K_L.C_e}$	$\frac{1}{q_e} = \frac{1}{q_m.K_L}\frac{1}{C_e} + \frac{1}{q_m}$	$\frac{1}{q_e}$ vs. $\frac{1}{C_e}$
Freundlich	$q_e = K_F.C_e^{1/n}$	$\ln q_e = \ln K_F + \frac{1}{n}\ln C_e$	$\ln q_e$ vs. $\ln C_e$
Temkin	$q_e = B_T(\ln A_T.C_e)$	$q_e = B_T(\ln C_e) + (B_T \ln A_T)$	q_e vs. $\ln C_e$
	$\theta = \frac{RT}{\Delta Q}\ln(K_T.C_e)$	$\theta = \frac{RT}{\Delta Q}\ln(C_e) + \frac{RT}{\Delta Q}\ln(K_T)$	θ vs. $\ln(C_e)$
Dubinin-Radushkevich	$\ln q_e = \ln q_s - \beta\varepsilon^2$	$\ln q_e = \ln q_s - \beta\varepsilon^2$	$\ln q_e$ vs. ε^2
Flory-Huggins	$\frac{\theta}{C_O} = K_{FH}(1-\theta)^{nFH}$	$\ln\left(\frac{\theta}{C_O}\right) = nFH\ln(1-\theta) + \ln K_{FH}$	$\ln\left(\frac{\theta}{C_O}\right)$ vs. $\ln(1-\theta)$
Fowler–Guggenheim	$K_{FG}.C_e = \frac{\theta}{1-\theta}\exp\left(\frac{2.\theta.W}{R.T}\right)$	$\ln\left(\frac{C_e(1-\theta)}{\theta}\right) = -\ln K_{FG} + \frac{2.\theta.W}{R.T}$	$\ln\left(\frac{C_e(1-\theta)}{\theta}\right)$ vs. θ
Hill-de Boer	$K_1.Ce = \frac{\theta}{1-\theta}\exp\left(\frac{\theta}{1-\theta} - \frac{K_2\theta}{RT}\right)$	$\ln\left(\frac{C_e(1-\theta)}{\theta}\right) - \frac{\theta}{1-\theta} = -\ln K_1 - \frac{K_2.\theta}{R.T}$	$\ln\left(\frac{C_e(1-\theta)}{\theta}\right) - \frac{\theta}{1-\theta}$ vs. θ

Figure 11 shows the plotting analysis based on the Dubinin-Radushkevich model. R^2 values for this model is the worst, informing that adsorption profile using carbon particles will not follow this model. Adsorption capacities q_s of the carbon particles are less than q_m gained from Langmuir model, in which the values cannot be guaranteed due to the less R^2 values. The analysis of E value in this model also confirmed that the process involved physical process for all cases.

Figure 12 shows the plotting analysis based on the Hill-de Boer model. R^2 values for this model is good for all particle sizes ($R^2 > 0.91$). This model is the most fitted model for particles with sizes of larger than 500 um, informing the involvement of multilayer structure in the adsorption process. The values of K_2 confirmed that there is some attractions among the adsorbed molecules.

Figure 13 shows the plotting analysis based on Fowler-Guggenheim model. R^2 values for this model is good for all particle sizes ($R^2 > 0.90$). The analysis of W values showed that the adsorbed molecules repulse each other and involve an endothermic reaction. The values of Gibbs energy from this K_{FG} also presented negative values, informing the spontaneous adsorption process

Figure 14 shows the plotting analysis based on the Flory-Huggins model. R^2 values for this model is less compared to other models. The analysis of number of molecules *nFH* confirmed the existence of interaction between adsorbed molecules and free molecules in the solution. The free molecules attached and interacted on the adsorbed molecules. The number of interacted molecules decreased with smaller carbon particle sizes. The values of the Gibbs free energy from this K_{FH} also presented negative values, informing the spontaneous adsorption process.

Table 2. Adsorption parameters based on standard isotherm models

A	Parameter	Particle size (µm)	Notes				
		1000	700	500	200	100	
Langmuir	q_m (mg/g)	10.58	14.26	36.00	35.15	38.68	The maximum monolayer adsorption capacity
	K_L (L/mg)	0.1469	0.0938	0.0276	0.0451	0.0634	Langmuir adsorption constant
	R_L	0.2700	0.3654	0.6567	0.5668	0.5150	$0 < R_L < 1$, indicating favorable adsorption.
	R^2	0.6081	0.8611	0.9883	0.9263	0.9045	The correlation coefficient.
	ΔGf (kJ/mol)	-36.50	-37.62	-40.65	-39.43	-38.59	$\Delta Gf < 0$, informing spontaneous process
Freundlich	N	2.5528	0.4634	1.3921	1.4189	1.5411	$n > 1$, defining adsorption with physical process.
	$1/n$	0.3917	0.4634	0.7183	0.7048	0.6489	$1/n = 0 – 1$, indicating favorable adsorption.
	k_f (mg/g)	2.4014	2.2656	1.4570	2.0405	3.1856	The Freundlich constant
	R^2	0.8083	0.9351	0.9961	0.9647	0.9469	The correlation coefficient.
	ΔGf (kJ/mol)	-29.58	-29.73	-30.82	-29.99	-28.88	$\Delta Gf < 0$, informing spontaneous process
Temkin	A_T (L/g)	0.6038	0.4532	0.2483	0.2662	0.3459	The equilibrium binding constant
	B_T (J/mol)	3.2232	4.2844	8.3780	10.8168	12.1335	Size > 500 um, $B_T < 8$ kJ, indicating physical adsorption
							Size < 500 um, $B_T > 8$ kJ, indicating chemical adsorption
	R^2 (eq.(5))	0.7775	0.8795	0.9630	0.8827	0.8721	The correlation coefficient from equation (5)
	K_T (L/mg)	0.0082	0.0057	0.0005	0.0005	0.0007	The Temkin constant
	ΔH (kJ/mol)	26.5750	28.3293	47.2500	38.0722	29.5521	$\Delta Gf > 0$, informing endothermic process
	R^2 (eq.(6))	0.8613	0.9258	0.9744	0.8183	0.8360	The correlation coefficient from equation (6)
Dubinin-Radushkevich	q_s (mg/g)	8.82	10.74	16.07	19.49	23.52	The maximum adsorption capacity of adsorbent.
	β (mol^2/kJ^2)	4.62	6.28	10.32	7.20	4.93	The Dubinin-Radushkevich isotherm saturation capacity
	E (kJ/mol)	0.3290	0.2823	0.2201	0.2636	0.3184	$E < 8$ kJ/mol, replying physical adsorption
	R^2	0.4020	0.6198	0.7979	0.6626	0.6442	The correlation coefficient
Hill-de Boer	K_1 (L/mg)	0.000659	0.000452	0.000045	0.000105	0.000112	Hill–de Boer constant
	K_2 (kJ/mol)	42.56	45.28	63.77	48.02	42.36	$K_2>0$, informing attraction between adsorbed molecules
	R^2	0.9446	0.9686	0.9862	0.9145	0.9385	The correlation coefficient
Fowler-Guggenheim	W (kJ/mol)	-19.27	-20.59	-29.67	-21.16	-17.53	$W < 0$, informing repulsion among adsorbed molecules and negative heat of adsorption
	K_{FG} (L/mg)	0.000703	0.000487	0.000051	0.000136	0.000184	Fowler–Guggenheim equilibrium constant
	R^2	0.9307	0.9607	0.9838	0.8908	0.9104	The correlation coefficient
Flory-Huggins	nFH	10	11	15	9	6	Number of adsorbates occupying on the surface site
	K_{FH} (L/mg)	0.000997	0.000739	0.000116	0.000411	0.000760	Flory-Huggins constant
	ΔGf (kJ/mol)	-17.12	-17.86	-22.46	-19.32	-17.79	$\Delta Gf < 0$, informing spontaneous process
	R^2	0.8853	0.9333	0.9763	0.8353	0.8391	The correlation coefficient

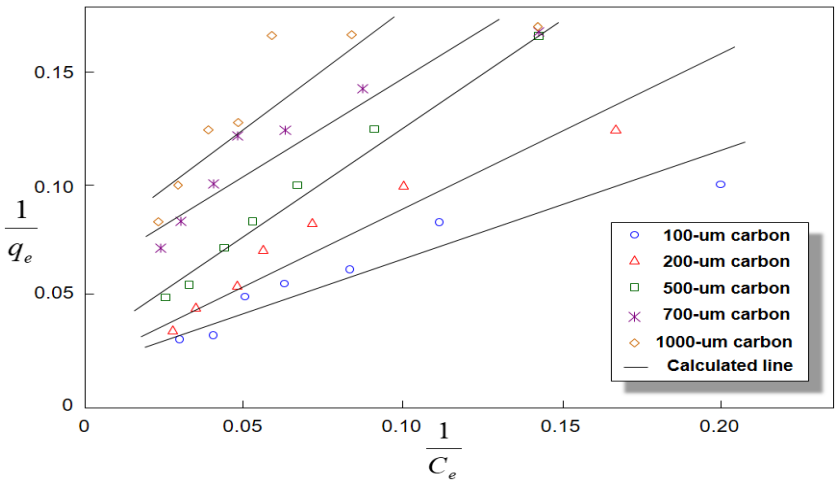

Figure 7. Isotherm adsorption of curcumin on various sizes of carbon microparticles using the Langmuir model

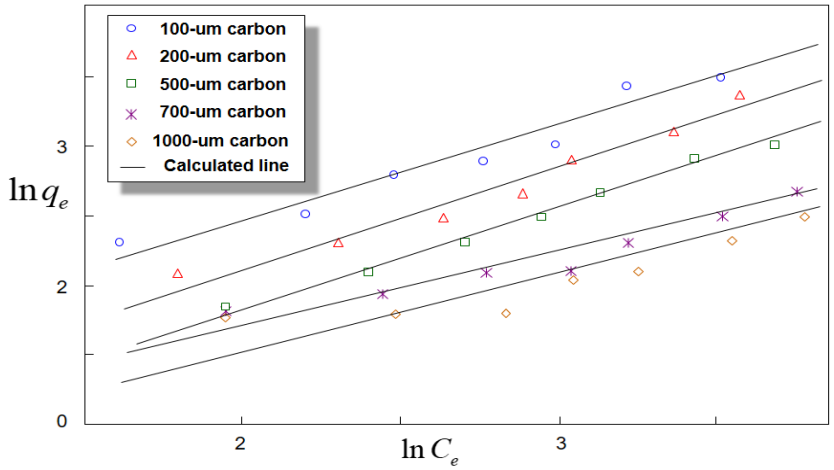

Figure 8. Isotherm adsorption of curcumin on various sizes of carbon microparticles using the Freundlich model

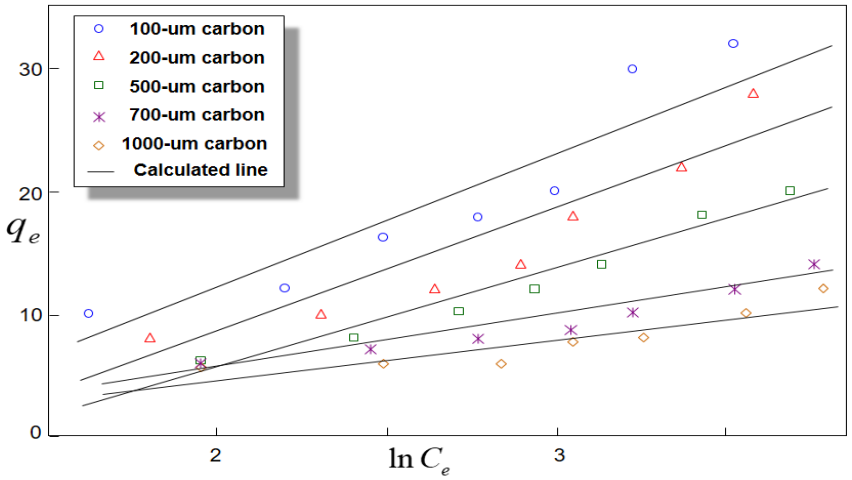

Figure 9. Isotherm adsorption of curcumin on various sizes of carbon microparticles using the Temkin model based on the amount of molecules adsorbed per gram at equilibrium.

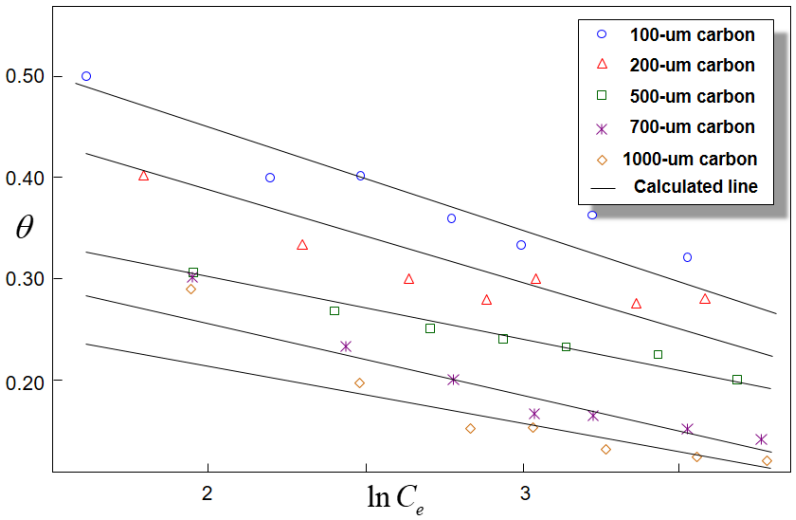

Figure 10. Isotherm adsorption of curcumin on various sizes of carbon microparticles using the Temkin model based on fraction of adsorbed component on the surface of adsorbent.

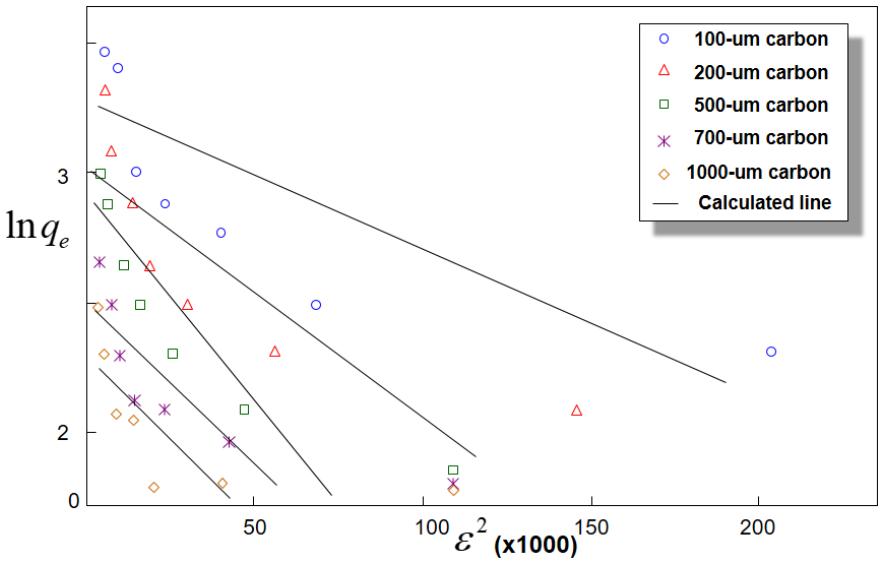

Figure 11. Isotherm adsorption of curcumin on various sizes of carbon microparticles using the Dubinin-Radushkevich model.

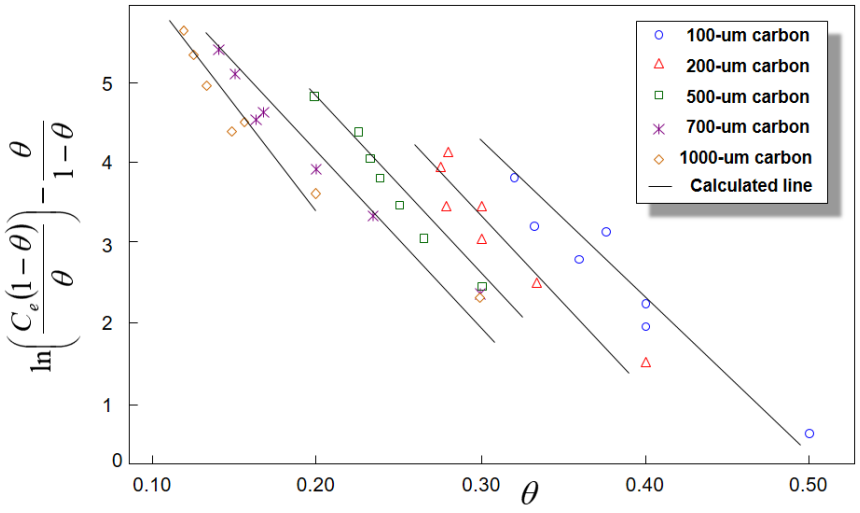

Figure 12. Isotherm adsorption of curcumin on various sizes of carbon microparticles using the Hill-de Boer model.

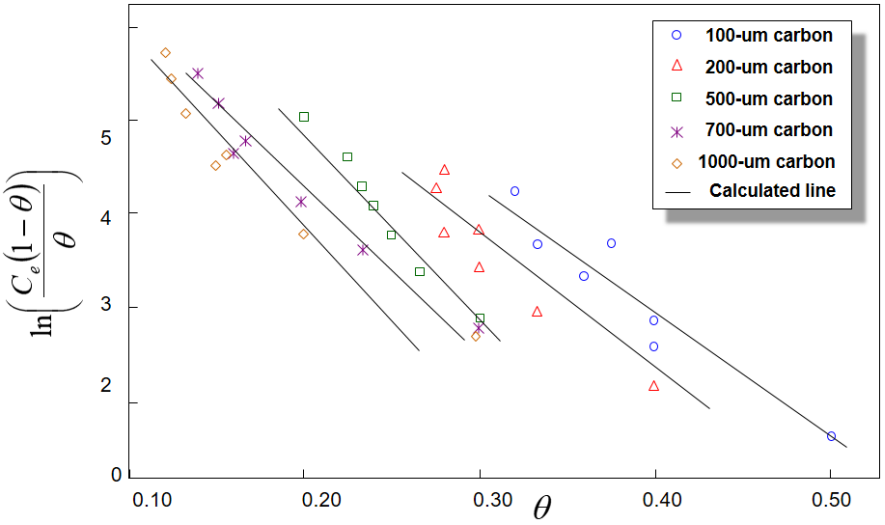

Figure 13. Isotherm adsorption of curcumin on various sizes of carbon microparticles using the Fowler-Guggenheim model.

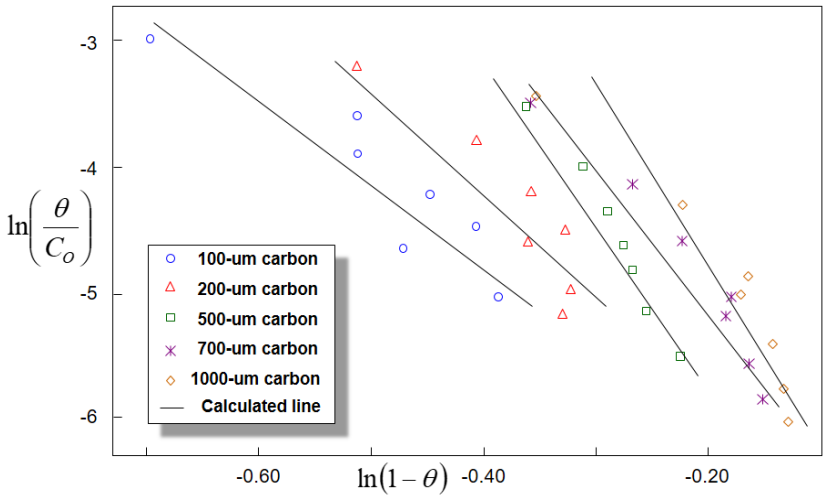

Figure 14. Isotherm adsorption of curcumin on various sizes of carbon microparticles using the Flory-Huggins model.

4. Discussion

The isotherm adsorption models (except for Dubinin – Radushkevich model) agree with the experimental results. The Gibbs free energy calculated is negative for all models, informing that the adsorption process done spontaneously. The analysis of the adsorption efficiency (η) and maximum adsorption capacity (q_m) (see **Figure 6**) implied that the increases in the adsorption sites have a direct correlation to the lowering the adsorbent sizes. The smaller particles have larger surface area, which in turn gives positive impact to the increases in the number of adsorption sites[19]. With increasing number of adsorption site, it increases the ability of adsorbent to adsorb more adsorbates on its surface area[6]. As shown in **Figure 6**, increases in the concentration have a negative impact on the efficiency of the adsorbent. This is because there is a limitation in number of active site for taking care of adsorbate molecules. Moreover, too much concentration of adsorbate can deter and blockage the adsorption of other molecules. The regression results from the data have almost identical gradient, but the intercept was different. Different values of intercepts are due to the effect of surface area on the adsorbent. In short, this confirms that smaller adsorbent sizes have larger surface area. The R^2 analysis confirmed that the isotherm adsorption depended on the particle sizes. In short, the isotherm adsorption profile can be divided into two categories: particle sizes of less than 500 um and larger

than 500 um. For the particles with sizes of less than 500 um, they followed Freundlich model (the highest R^2 values), informing that the adsorption involves is done in multilayer structure[19]. The adsorption between adsorbate molecules and surface of adsorbent is a physical interaction, and the adsorption is favorable (controllable adsorption, depending on the process condition). The model of multilayer is also confirmed by the Hill-de Boer model (confirmed by high values of R^2 in this model). K_2 values identified that the attraction between adsorbed molecules on the adsorbent and free molecules in the solution. The Langmuir model has good R^2 values for particles with sizes of less than 500 um, informing that the adsorption of molecules distribute on all surfaces of adsorbent. The molecules diffuse from liquid phase on the solid phase on the surface of adsorbent[33]. The number of adsorbate molecules on the surface of adsorbent can be described by R_L value[9], in which the results of R_L values are between 0 and 1, showing the normal favorable adsorption process (the adsorption is controllable by changing the process condition). The Fowler–Guggenheim model confirmed the repulsion among adsorbed molecules. The less R^2 values were found for the Temkin and the Flory-Huggins models. However, the models confirmed the physical adsorption process (which is in line with n value in the Freundlich model) and the number of occupying adsorbate on the surface active site (which is in a good agreement with the K_2 values in the Hill-de Boer model). The particles with sizes of larger than 500 um followed the Hill-de Boer model, confirming the multilayer structure and attraction of adsorbate molecules and free molecules. The interaction between adsorbed molecule and free molecule is confirmed by the Flory-Huggins model. The Fowler–Guggenheim model confirmed repulsion phenomena between adsorbed molecules. Different from carbon microparticles with sizes of less than 500 um, larger particles are not fit with Langmuir and Temkin models. Although the trends in the models that fit with the experimental results, all models agree that the adsorption profile follow the multilayer adsorption with a physical adsorption, in which the illustration phenomena in the adsorption process is shown in **Figure 15**. All sites on the adsorbent are active for taking care of adsorbed molecules (see part (a) in **Figure 15**) from free molecules in the solution (see part (b) in **Figure 15**). The condition of multilayer with no interaction between adsorbed molecules is due to the existence of surface structure on the surface of adsorbent (see part (b) in **Figure 15**). The adsorbate molecules contacts each other to form multilayer (see part (c) in **Figure 15**), and they attach on the surface of adsorbent separately (i.e. there is no interaction each other between adsorbed molecules; see part (d) in **Figure 15**)). Then, the porous structure promotes more adsorption and prevents desorption process. As discussed in **Figure 3**, the production of carbon microparticles from the pumpkin seeds results in the formation of porosity in the product. Organic components are converted into carbon, whereas inorganic components form metal oxide. When we applied etching process into the composite, the carbon components remains and metal oxide removes. The pores themselves are from the releases of inorganic components. Since pumpkin seeds have inorganic content of about 3% [34], the formed pores will be in micro- to meso-pores structure (less than 2 nm)[6]. The existence pores have two advantages: (1) enlarging surface active sites (as shown in the increases in the adsorption efficiency η as decreases in particle size), and (2) surface structure (increases number of adsorption process, trapping molecules inside the pores and decreasing number of desorption process).

4. Conclusion

This study has successfully evaluated the isotherm adsorption of carbon microparticles with various sizes (from 100 to 1000 um) prepared from pumpkin (*Cucurbita maxima*) seeds using seven isotherm models. The models (i.e. Langmuir, Freundlich, Temkin, Dubinin-Radushkevich, Flory-Huggins, Fowler–Guggenheim, and Hill-de Boer isotherm models) were used to predict and determine the characteristic parameters. The results showed that the interaction of adsorbates with carbon surface is done in multilayers with physical processes. Inorganic contents in the pumpkin seeds allow the formation of carbon with porosities, making more sites for the adsorption. The adsorbed

molecules attract and associate with other free adsorbate molecules. The adsorption is carried out on energetically different sites under an endothermic process. The Gibbs free energy confirmed that the adsorption is spontaneous. The results also confirmed that smaller adsorbents have direct impacts on the improving adsorption capacities (due to the existence of large surface area). Small-sized adsorbent (sizes < 500 um) has better additional adsorption (due to adsorbate-adsorbate interaction and possible existence of chemical interaction), resulting in the boosting adsorption capacity. This study is useful for further developments of carbon microparticles from organic waste material.

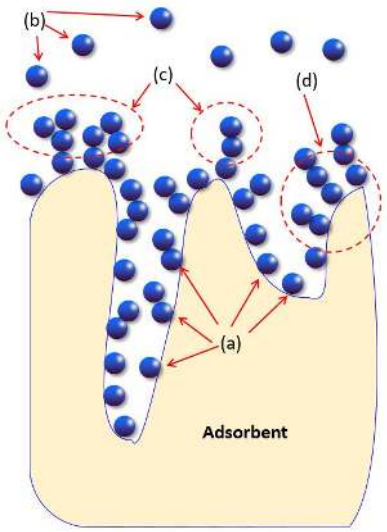

Figure 15. Proposal illustration of adsorption profile of carbon microparticles in adsorbing adsorbate molecules. (a), (b), (c), and (d) are the adsorbed molecule on the surface active; interaction between adsorbed and free molecules; individual adsorbed molecules in their surface site (separated each other); and free molecules, respectively.

Acknowledgements- This study acknowledged RISTEK BRIN for Grant-in-aid Penelitian Terapan (PT) and Penelitian Terapan Unggulan Perguruan Tinggi (PTUPT).

References

[1] F. Yan, Z. Sun, H. Zhang, X. Sun, Y. Jiang, Z. Bai The fluorescence mechanism of carbon dots, and methods for tuning their emission color: A review, *Microchimica Acta*, 186(8) (2019), 583.

[2] H. K. Sharma, C. Xu, W. Qin Biological pretreatment of lignocellulosic biomass for biofuels and bioproducts: an overview, *Waste and Biomass Valorization*, 10(2) (2019), 235-251.

[3] I. Demiral, C. Aydın Şamdan, H. Demiral Production and characterization of activated carbons from pumpkin seed shell by chemical activation with ZnCl2, *Desalination and Water Treatment*, 57(6) (2016), 2446-2454.

[4] J. Rosas, J. Bedia, J. Rodríguez-Mirasol, T. Cordero On the preparation and characterization of chars and activated carbons from orange skin, *Fuel Processing Technology*, 91(10) (2010), 1345-1354.

[5] A. Dada, A. Olalekan, A. Olatunya, O. Dada Langmuir, Freundlich, Temkin and Dubinin–Radushkevich isotherms studies of equilibrium sorption of Zn2+ unto phosphoric acid modified rice husk, *IOSR Journal of Applied Chemistry*, 3(1) (2012), 38-45.

[6] A. B. D. Nandiyanto, Z. A. Putra, R. Andika, M. R. Bilad, T. Kurniawan, R. Zulhijah, et al. Porous activated carbon particles from rice straw waste and their adsorption properties, *Journal of Engineering Science and*

Technology, 12 (2017), 1-11.
[7] A. Sukmafitri, R. Ragadhita, A. B. D. Nandiyanto, W. C. Nugraha, B. Mulyanti Effect of ph condition on the production of well-dispersed carbon nanoparticles from rice husks, *Journal of Engineering Science and Technology*, 15(2) (2020), 991-1000.
[8] A. M. Anshar, P. Taba, I. Raya Kinetic and thermodynamics studies the adsorption of phenol on activated carbon from rice husk activated by ZnCl2, *Indonesian Journal of Science and Technology*, 1(1) (2016), 47-60.
[9] R. Ragadhita, A. B. D. Nandiyanto, W. C. Nugraha, A. Mudzakir Adsorption isotherm of mesopore-free submicron silica particles from rice husk, *Journal of Engineering Science and Technology*, 14(4) (2019), 2052-2062.
[10] I. I. Gurten, M. Ozmak, E. Yagmur, Z. Aktas Preparation and characterisation of activated carbon from waste tea using K2CO3, *Biomass and Bioenergy*, 37 (2012), 73-81.
[11] A. H. Jawad, A. M. Kadhum, Y. Ngoh Applicability of dragon fruit (Hylocereus polyrhizus) peels as low-cost biosorbent for adsorption of methylene blue from aqueous solution: kinetics, equilibrium and thermodynamics studies, *Desalin Water Treat*, 109 (2018), 231-240.
[12] J. Yang, K. Qiu Preparation of activated carbons from walnut shells via vacuum chemical activation and their application for methylene blue removal, *Chemical Engineering Journal*, 165(1) (2010), 209-217.
[13] A. Okoye, P. Ejikeme, O. Onukwuli Lead removal from wastewater using fluted pumpkin seed shell activated carbon: Adsorption modeling and kinetics, *International Journal of Environmental Science & Technology*, 7(4) (2010), 793-800.
[14] W. C. Lim, C. Srinivasakannan, N. Balasubramanian Activation of palm shells by phosphoric acid impregnation for high yielding activated carbon, *Journal of Analytical and Applied Pyrolysis*, 88(2) (2010), 181-186.
[15] A. L. Cazetta, A. M. Vargas, E. M. Nogami, M. H. Kunita, M. R. Guilherme, A. C. Martins, et al. NaOH-activated carbon of high surface area produced from coconut shell: Kinetics and equilibrium studies from the methylene blue adsorption, *Chemical Engineering Journal*, 174(1) (2011), 117-125.
[16] U. Haura, F. Razi, H. Meilina Karakterisasi Adsorben dari Kulit Manggis dan Kinerjanya pada Adsorpsi Logam Pb (II) dan Cr (VI)-(Adsorbent Characterization from Mangosteen Peel and Its Adsorption Performance on Pb (II) and Cr (VI)), *Biopropal Industri*, 8(1) (2017), 47-54.
[17] J. Hmimou, S. Elanza, E. Rifi, A. Lebkiri, M. E. Touhami, Z. Hatim Equilibrium and Kinetic Modeling of Zn (II) Adsorption from aqueous solution using dicalcique dehydrated, *Moroccan Journal of Chemistry*, 3(2) (2015), 3-2 (2015) 263-271.
[18] M. Morad, M. Hilali, L. Bazzi, A. Chaouay Adsorption of organic molecule (acetic acid) on activated carbon in aqueous, *Moroccan Journal of Chemistry*, 2(5) (2014), 2-5 (2014) 475-485.
[19] M. Fiandini, R. Ragadhita, A. B. D. Nandiyanto, W. C. Nugraha Adsorption characteristics of submicron porous carbon particles prepared from rice husk, *Journal of Engineering Science and Technology*, 15(1) (2020), 022-031.
[20] A. K. Dhiman, K. Sharma, S. Attri Functional constitutents and processing of pumpkin: A review, *Journal of Food Science and Technology*, 46(5) (2009), 411.
[21] W. Morgan, D. Midmore Kabocha and Japanese pumpkin in Australia, *Rural Industries Research and Development Corporation Publication*, 2 (2003), 167.
[22] N. Permatasari, T. N. Sucahya, A. B. D. Nandiyanto Agricultural wastes as a source of silica material, *Indonesian Journal of Science and Technology*, 1(1) (2016), 82-106.
[23] I. Langmuir The adsorption of gases on plane surfaces of glass, mica and platinum, *Journal of the American Chemical society*, 40(9) (1918), 1361-1403.
[24] H.-K. Chung, W.-H. Kim, J. Park, J. Cho, T.-Y. Jeong, P.-K. Park Application of Langmuir and Freundlich

isotherms to predict adsorbate removal efficiency or required amount of adsorbent, *Journal of Industrial and Engineering Chemistry*, 28 (2015), 241-246.
[25] J. Romero-Gonzalez, J. R. Peralta-Videa, E. Rodrıguez, S. L. Ramirez, J. L. Gardea-Torresdey Determination of thermodynamic parameters of Cr (VI) adsorption from aqueous solution onto Agave lechuguilla biomass, *The Journal of chemical thermodynamics*, 37(4) (2005), 343-347.
[26] N. Ayawei, A. N. Ebelegi, D. Wankasi Modelling and interpretation of adsorption isotherms, *Journal of Chemistry*, 2017 (2017), 3039817.
[27] R. Saadi, Z. Saadi, R. Fazaeli, N. E. Fard Monolayer and multilayer adsorption isotherm models for sorption from aqueous media, *Korean Journal of Chemical Engineering*, 32(5) (2015), 787-799.
[28] O. Hamdaoui, E. Naffrechoux Modeling of adsorption isotherms of phenol and chlorophenols onto granular activated carbon: Part I. Two-parameter models and equations allowing determination of thermodynamic parameters, *Journal of hazardous materials*, 147(1-2) (2007), 381-394.
[29] B. Ali Fil, M. Korkmaz, G. Özmetin An empirical model for adsorption thermodynamics of copper (II) from solutions onto illite clay-batch process design, *Journal of the Chilean Chemical Society*, 59(4) (2014), 2686-2691.
[30] A. B. D. Nandiyanto, R. Andika, M. Aziz, L. S. Riza Working volume and milling time on the product size/morphology, product yield, and electricity consumption in the ball-milling process of organic material, *Indonesian Journal of Science and Technology*, 3(2) (2018), 82-94.
[31] A. B. D. Nandiyanto, D. Sofiani, N. Permatasari, T. N. Sucahya, A. S. Wiryani, A. Purnamasari, et al. Photodecomposition profile of organic material during the partial solar eclipse of 9 march 2016 and its correlation with organic material concentration and photocatalyst amount, *Indonesian Journal of Science and Technology*, 1(2) (2016), 132-155.
[32] A. B. D. Nandiyanto, R. Oktiani, R. Ragadhita How to Read and Interpret FTIR Spectroscope of Organic Material, *Indonesian Journal of Science and Technology*, 4(1) (2019), 97-118.
[33] E. Voudrias, K. Fytianos, E. Bozani Sorption–desorption isotherms of dyes from aqueous solutions and wastewaters with different sorbent materials, *Global Nest International Journal*, 4(1) (2002), 75-83.
[34] L. Rezig, M. Chouaibi, K. Msaada, S. Hamdi Chemical composition and profile characterisation of pumpkin (Cucurbita maxima) seed oil, *Industrial Crops and Products*, 37(1) (2012), 82-87.